Noisy Werner-Holevo channel and its properties

Shayan Roofeh and Vahid Karimipour
Department of Physics, Sharif University of Technology, P.O. Box 11155-9161, Tehran, Iran

(Received 15 November 2023; accepted 29 April 2024; published 14 May 2024)

Interest in the Werner-Holevo channel $\Lambda_1(\rho) = \frac{1}{2}[\mathrm{tr}(\rho)I - \rho^T]$ has been mainly due to its abstract mathematical properties. We show that in three dimensions and with a slight modification, this channel can be realized as the rotation of qutrit states in random directions by random angles. Our modification takes the form $\Lambda_x(\rho) = (1-x)\rho + x\Lambda_1(\rho)$. Therefore, and in view of the potential use of qutrits in quantum processing tasks and their realization in many different platforms, the modified Werner-Holevo channel can be used as a very simple and realistic noise model, in the same way that the depolarizing channel is for qubits. We will make a detailed study of this channel and derive its various properties. In particular, we will use the recently proposed flag extension and other techniques to derive analytical expressions and bounds for the different capacities of this channel. The role of symmetry is revealed in these derivations. We also rigorously prove that the channel Λ_x is antidegradable and hence has zero quantum capacity, in the region $\frac{4}{7} \leqslant x \leqslant 1$.

DOI: 10.1103/PhysRevA.109.052620

I. INTRODUCTION

A quantum state is a matrix that is Hermitian, positive, and of unit trace. Any operation which is quantum mechanically conceivable should preserve these basic properties. Nevertheless the familiar operation of transposing a matrix $\rho \longrightarrow \rho^T$, which for qubits is equivalent to converting any pure state to its orthogonal $|\psi\rangle \longrightarrow |\psi^T\rangle$, while having all these properties is not a feasible quantum operation and cannot be implemented in any physical process. The reason is that it lacks the important and extra property of complete positivity, which is required to ensure that local actions on parts of a larger system also retain properties of quantum states. While transposing a quantum state is forbidden, it was interestingly shown in Ref. [1] that in any dimensions d, the so-called Werner-Holevo map

$$\rho \longrightarrow \Lambda_{\mathrm{WH}}(\rho) = \frac{1}{d-1}[\mathrm{tr}(\rho)\mathbb{I} - \rho^T], \tag{1}$$

despite the presence of the negative sign and the transpose, is indeed a completely positive trace-preserving map. For qubits, it is no surprise that such a map is a physical operation since given a density matrix $\rho = \begin{pmatrix} a & b \\ b^* & c \end{pmatrix}$, we simply have

$$\Lambda_{\mathrm{WH}}(\rho) = \begin{pmatrix} c & -b^* \\ -b & a \end{pmatrix} = \sigma_y \rho \sigma_y, \tag{2}$$

which implies that a unitary operation, i.e., a rotation around the y axis by 180°, covers ρ to $\mathrm{tr}\rho\mathbb{I} - \rho^T$. For qutrits, however, the Werner-Holevo channel is no longer a unitary map, as simply as in the qubit case, but it is still possible to show that it is an acceptable quantum operation. The reason is that it has an explicit Kraus representation which proves that it is indeed a completely positive trace-preserving (CPT) map. In fact, it is known that [2]

$$\Lambda_{\mathrm{WH}}(\rho) = \tfrac{1}{2}[\mathrm{tr}(\rho)\mathbb{I} - \rho^T] = \tfrac{1}{2}(J_x\rho J_x + J_y\rho J_y + J_z\rho J_z), \tag{3}$$

where J_x, J_y, and J_z are the spin-1 representations of angular momentum algebra, i.e.,

$$J_x = -i\begin{bmatrix} 0 & 0 & 0 \\ 0 & 0 & 1 \\ 0 & -1 & 0 \end{bmatrix},\quad J_y = -i\begin{bmatrix} 0 & 0 & -1 \\ 0 & 0 & 0 \\ 1 & 0 & 0 \end{bmatrix},\quad J_z = -i\begin{bmatrix} 0 & 1 & 0 \\ -1 & 0 & 0 \\ 0 & 0 & 0 \end{bmatrix}. \tag{4}$$

When written in this form, the channel is a special case of the more general types of channels called the Landau-Streater channel [3].[1] The importance of the equivalence of the Werner-Holevo with the Landau-Streater channel for qutrits is beyond a simple depiction of the Kraus representation for the former channel. In fact, as has been shown in Ref. [3], here we are dealing with the first example of a unital channel which cannot be realized as a collection of random unitary operations. More concretely, the map Λ_{WH}, while having the property $W_{\mathrm{WH}}(I) = I$, cannot be written as $\Lambda_{\mathrm{WH}}(\rho) = \sum_i p_i U_i \rho U_i^\dagger$ for any choice of unitary actions and any choice of randomness. This means that the map Λ_{WH} cannot be realized as the random unitary operations (jumps) on the qutrit as it travels along in time or space. It cannot even be written as the convex combination of two other maps. In other words, it is an extreme point in the space of qutrit channels. This is an intriguing result since it is well known that for qubits, any unital map can be written as a random

[1] For higher dimensions, the Kraus operators are the spin-j representation of the angular momentum algebra and the factor $\frac{1}{2}$ should be replaced with $\frac{1}{j(j+1)}$.

unitary channel [4]. Furthermore, the Werner-Holevo channel (3) is not continuously connected to the identity channel, i.e., by a parameter which can be tuned to model the effect of environmental noise.

It is the aim of the present paper to show that by a small modification, that is, by combining it with the identity channel, this map can in fact be a sensible model of noise on qutrits. We will show that the resulting model, defined as

$$\Lambda_x(\rho) = (1-x)\rho + x\Lambda_{\rm WH}(\rho) = (1-x)\rho - \frac{x}{2}\rho^T + \frac{x}{2}{\rm tr}(\rho)\mathbb{I} \quad 0 \leqslant x \leqslant 1, \tag{5}$$

as long as $x \neq 1$, can in fact be represented as a model in which the environmental noise randomly rotates the qutrit by small angles in arbitrary directions, where the parameter x is determined by the probability distribution of random rotations.

This result is significant in several respects: First, from the practical point of view, while universal quantum computing has been conventionally based on qubits, there are many attempts to explore the potential advantages [5–11] and physical realization of higher-dimensional systems, especially qutrits. The latter ranges from orbital angular momentum of light [12–15] and other photonic platforms [7,16–24] to NMR ensembles, [25] superconducting quantum circuits [26–30], and trapped ions [18,26,31–34].

Second, the channel Λ_x defined in (5) plays the same role for qutrits as the depolarizing channel plays for qubits. It is true that the conventional depolarizing channel for qutrits, $\rho \longrightarrow (1-p)\rho + \frac{p}{3}I$, allows a random unitary representation in terms of Heisenberg-Weyl operators [35]. However, the Kraus or the error operators of this channel, while being unitary, are discrete operators which are not connected with the identity operator by a continous parameter representing the level of noise. The level of noise is controlled by the parameter p for all these Kraus operators. Therefore, it seems that the channel Λ_x shows a more natural type of noise in many practical and numerical studies of qutrit systems. In particular, it may have relevance to quantum processes involving the quantum Zeno effect [36], where a series of measurements can slow down the quantum dynamics [37–40] or a series of small rotations and measurements can activate bound entanglement [41] in qutrit states [42]. Finally, from a mathematical point of view, this result may encourage others to study the vicinity of extreme points of quantum channels in general.

After proving this physical realization, we will proceed to investigate many of the other properties of the channel. In particular, we will examine the symmetry properties of the channel and the way it affects the most important properties of the channel, namely, its various kinds of capacities. As a prerequisite to this investigation, we will study the so-called degradability and antidegradability [43] conditions for the channel. Equipped with these tools and exploiting the flag extensions [44,45] of the channel, we are able to find exact expressions for the Holevo quantity of the channel, the entanglement-assisted capacity of the channel, and finally upper and lower bounds for the quantum capacity. Finally, we rigorously prove that the channel Λ_x is antidegradable and hence has zero quantum capacity, in the region $\frac{4}{7} \leqslant x \leqslant 1$.

The structure of this paper is as follows: In Sec. (II), we show that the channel Λ_x is indeed a random unitary channel and show that random rotations of an input qutrit state distort the qutrit in the way suggested by (5). In Sec. (III), we study the structural properties of this channel, its spectrum, and its complementary channel. In Sec. (IV), we extend this study to the important problem of degradability and antidegradability, which is an important requirement for the calculation of various capacities of the channel. In Sec. (V), we use everything we have learned in previous sections to study various capacities of this channel and provide exact expressions or upper and lower bounds for these capacities. Finally, in Sec. (VI), we prove that the channel Λ_x is antidegradable and hence has zero quantum capacity, in the region $\frac{4}{7} \leqslant x \leqslant 1$. We conclude the paper with a summary and outlook.

II. THE RANDOM ROTATION MODEL

Consider a qutrit state ρ passing through a communication channel, either in time or in space, and undergoing random kicks (rotations in random directions by random angles). The output state will then be of the form

$$\Phi(\rho) = \int d\mathbf{n} d\theta P(\mathbf{n}, \theta) e^{i\mathbf{n}\cdot\mathbf{J}\theta} \rho e^{-i\mathbf{n}\cdot\mathbf{J}\theta}, \tag{6}$$

where $P(\mathbf{n}, \theta)$ is the probability density of a rotation being around the direction $\mathbf{n}$ by an angle $-\frac{\pi}{2} \leqslant \theta \leqslant \frac{\pi}{2}$. We will take this distribution to be uncorrelated in direction and angle. Moreover, in the absence of any preference, we take the distribution in directions to be uniform, hence $P(\mathbf{n}, \theta) = \frac{1}{4\pi}P(\theta)$. It is also natural to assume an even distribution function for angles, that is, $P(\theta) = P(-\theta)$. We will now use the identity for spin-1 representation (4)

$$e^{i\mathbf{n}\cdot\mathbf{J}\theta} = 1 + i\sin\theta\, \mathbf{n}\cdot\mathbf{J} + (\cos\theta - 1)(\mathbf{n}\cdot\mathbf{J})^2, \tag{7}$$

which in view of $P(\theta) = P(-\theta)$ is simplified to

$$\Lambda(\rho) = \rho + \langle\cos\theta - 1\rangle[\rho\langle\mathbf{n}\cdot\mathbf{J})^2 + \langle\mathbf{n}\cdot\mathbf{J}\rangle^2\rho] + \langle\sin^2\theta\rangle\langle\mathbf{n}\cdot\mathbf{J}\rho\mathbf{n}\cdot\mathbf{J}\rangle + \langle(\cos\theta - 1)^2\rangle \times \langle(\mathbf{n}\cdot\mathbf{J})^2\rho(\mathbf{n}\cdot\mathbf{J})^2\rangle, \tag{8}$$

where $\langle f(\theta)\rangle := \frac{1}{2\pi}\int P(\theta)f(\theta)d\theta$ and $\langle f(\mathbf{n})\rangle := \frac{1}{4\pi}\int d\mathbf{n} f(\mathbf{n})$. We now use the well-known results on the average of unit vectors with uniform distributions to arrive at

$$\langle(\mathbf{n}\cdot\mathbf{J})^2\rangle = \langle n_i n_j\rangle J_i J_j = \tfrac{1}{3}J_i J_j = \tfrac{2}{3}\mathbb{I}, \tag{9}$$

where we have used the identity $J_x^2 + J_y^2 + J_z^2 = 2\mathbb{I}$. Moreover, we find

$$\langle\mathbf{n}\cdot\mathbf{J}\rho\mathbf{n}\cdot\mathbf{J}\rangle = \langle n_i n_j\rangle J_i\rho J_j = \frac{1}{3}\sum_i J_i\rho J_i = \frac{2}{3}\Lambda_{\rm WH}(\rho). \tag{10}$$

The other term that we should calculate is

$$\langle(\mathbf{n}\cdot\mathbf{J})^2\rho(\mathbf{n}\cdot\mathbf{J})^2\rangle = \langle n_i n_j n_k n_l\rangle J_i J_j \rho J_k J_l. \tag{11}$$

Using the identity

$$\langle n_i n_j n_k n_l\rangle = \tfrac{1}{15}(\delta_{ij}\delta_{kl} + \delta_{ik}\delta_{jl} + \delta_{il}\delta_{jk}) \tag{12}$$

and inserting the expression $J_i J_j = \delta_{ij}\mathbb{I} - |j\rangle\langle i|$, which is obtained from (4), it is straigthforward to simplify the expression

(11). The result is

$$\langle(\mathbf{n}\cdot\mathbf{J})^2\rho(\mathbf{n}\cdot\mathbf{J})^2\rangle = \tfrac{2}{5}\rho + \tfrac{1}{15}\rho^T + \tfrac{1}{15}\mathrm{tr}(\rho)\mathbb{I}. \tag{13}$$

Putting everything together, the final result is

$$\Phi(\rho) = a\rho - b\rho^T + \frac{1-a+b}{3}\mathrm{tr}(\rho)\mathbb{I}, \tag{14}$$

where

$$a = \tfrac{1}{15}\langle 1 + 8\cos\theta + 6\cos^2\theta\rangle,$$
$$b = \tfrac{1}{15}\langle 4 + 2\cos\theta - 6\cos^2\theta\rangle. \tag{15}$$

This shows that random unitary kicks do indeed produce the transpose of ρ with a negative sign, which is the characteristic of the Werner-Holevo channel, but they also produce the state ρ itself. Note that b is always positive, and a can never be zero, proving that the original Werner-Holevo channel, or equivalently the Landau-Streater channel, is indeed an extreme point in the space of qutrit channels. In fact, the minimum value of a is $\frac{1}{15} = 0.067$, which happens when all rotation angles are fixed at $\theta = \pm\frac{\pi}{2}$. This implies that the close vicinity of the channel Λ_{WH} is still not representable by random rotations. This of course does not exclude the possibility that this neighborhood be realized by other random unitary ensembles. The answer to this question is not yet known. When the random angles of rotation are very small so that we can neglect $\langle\theta^4\rangle$ and higher orders, the channel will take the form

$$\Phi(\rho) \approx \left(1 - \tfrac{2}{3}\langle\theta^2\rangle\right)\rho - \tfrac{1}{3}\langle\theta^2\rangle\rho^T + \tfrac{1}{3}\langle\theta^2\rangle\mathrm{tr}(\rho)\mathbb{I}, \tag{16}$$

which is nothing but the channel Λ_x (3) with $x = \frac{2}{3}\langle\theta^2\rangle$.

We now turn to the study of other properties of our channel and start with a remark on notations and conventions.

III. THE SYMMETRIES OF THE CHANNEL AND ITS SPECTRUM

We first set up our notations and conventions:

Notations and conventions: Let H_d be a d-dimensional Hilbert space; by $L(H_d)$, we mean the space of linear operators; by $L^+(H_d)$, the set of positive semi-definite operators; and by $D(H_d)$, the set of unit trace positive operators on H_d. d-dimensional square matrices are denoted by M_d and d-dimensional identity matrix by I_d. We employ the notation Φ to denote an arbitrary quantum channel, which is utilized in various contexts and definitions. For brevity of notations, we sometimes denote a system and its space of operators by the same letter. Therefore, a quantum map $\Phi : A \longrightarrow B$ is a shorthand for $\Phi : L(H_A) \longrightarrow L(H_B)$. Although the Landau-Streater channel is defined for spin-j, in this work, we exclusively study the channel for spin-1, which we refer to mostly as the Werner-Holevo channel, since they are equivalent. The channel Λ_{WH}, which in the notation used in (3) should be denoted by Λ_1, is obviously covariant in the following sense:

$$\Lambda_1(U\rho U^\dagger) = U^*\Lambda_1(\rho)U^{*\dagger}, \quad \forall\ U \in \mathrm{SU}(3). \tag{17}$$

Moreover, as we will see in Sec. (IV), it is both degradable and antidegradable, which implies that it has zero quantum capacity. That is, it cannot convey any quantum information at all. For a detailed treatment, see Ref. [46]. To see the covariance properties of the channel Λ_x, we note that since the density matrix ρ transforms as $\rho \longrightarrow U\rho U^\dagger$ and ρ^T transforms as $U^*\rho U^T$, the covariance of the channel Λ_x reduces from the group SU(3) to its smaller subgroup SO(3),

$$\Lambda_x(U\rho U^\dagger) = U\Lambda_x(\rho)U^\dagger, \quad \forall U \in \mathrm{SO}(3). \tag{18}$$

A. Spectral properties of the channel

The eigenvectors and eigenvalues of the channel can easily be found by noting that for any symmetric matrix, $\rho = \rho^T$, and for any antisymmetrix matrix, $\rho = -\rho^T$. Defining the diagonal matrices, $Z_1 =: E_{11} - E_{33}$ and $Z_2 =: E_{22} - E_{33}$, and the Hermitian matrices, $X_{sr} := E_{sr} + E_{sr}$ and $Y_{sr} := -i(E_{sr} - E_{sr})$ for $s < r$, where $E_{kl} = |k\rangle\langle l|$ is the matrix with one on its $k-l$ entry and zero otherwise, we find

$$\Lambda_x(I_3) = I_3, \quad \Lambda_x(Z_1) = \left(1 - \frac{3x}{2}\right)Z_1,$$
$$\Lambda_x(Z_2) = \left(1 - \frac{3x}{2}\right)Z_2,$$
$$\Lambda_x(X_{sr}) = \left(1 - \frac{3x}{2}\right)X_{sr}, \quad \Lambda_x(Y_{sr}) = \left(1 - \frac{x}{2}\right)Y_{sr}. \tag{19}$$

Counting the degeneracies of the eigenvalues, this shows that the determinant of the channel is equal to

$$\mathrm{Det}(\Lambda_x) = \left(1 - \frac{x}{2}\right)^3\left(1 - \frac{3}{2}x\right)^5. \tag{20}$$

This shows that the determinant of the channel is negative in a certain range, namely,

$$\mathrm{Det}(\Lambda_x) < 0, \quad \tfrac{2}{3} < x \leqslant 1. \tag{21}$$

In this range, the channel is not infinitely divisible and does not represent a Markovian evolution [47]. The question remains whether, within the range of $0 \leqslant x \leqslant \frac{2}{3}$, the channel can be described as the exponential of Lindbladian dynamics. We will explore this question in our future work.

B. Complementary channel

1. *Definition and covariance of complementary channel*

The concept of the complement of a channel hinges on the well-known Stinespring's dilation theorem [48], which states that a quantum channel $\Phi : A \longrightarrow B$ can be constructed as a unitary map $U : A \otimes E \longrightarrow B \otimes E'$, where E and E' are the environments of A and B, respectively. More formally, we have

$$\Phi(\rho) = \mathrm{tr}_{E'}(U\rho U^\dagger), \tag{22}$$

where U denotes an isometry mapping from A to $B \otimes E'$. In this configuration, the complementary channel $\Phi^c : A \longrightarrow E'$ is defined by

$$\Phi^c(\rho) = \mathrm{tr}_B(U\rho U^\dagger), \tag{23}$$

constituting a mapping from the input system to the output environment [see Fig. 1]. It is important to note that the complement of a quantum channel is not unique, but there exists a connection between them through isometries, as detailed

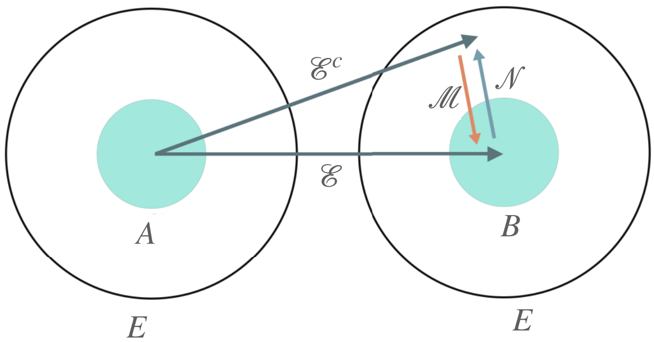

FIG. 1. The channel $\mathcal{E}$, its complement $\mathcal{E}^c$, and the channels $\mathcal{M}$ and $\mathcal{N}$, in the definition (1) of degradability and antidegradability. For simplicity, we have taken the environments of A and B, the same as E. In principle, they can be different.

in Ref. [49]. The Kraus operators of the channel Φ and its complement Φ^c are related as follows [50]:

$$\Phi(\rho) = \sum_\alpha K_\alpha \rho K_\alpha^\dagger,$$
$$\Phi^c(\rho) = \sum_i R_i \rho R_i^\dagger,$$
$$(R_i)_{\alpha,j} = (K_\alpha)_{i,j}. \tag{24}$$

As shown in Ref. [51], the covariance of a channel also induces a covariance on the complementary channel. The theorem of Ref. [51] states that if a channel Φ is covariant in the form

$$\Phi[U(g)\rho U^\dagger(g)] = V(g)\Phi(\rho)V^\dagger(g) \quad \forall\, g \in G, \tag{25}$$

where $U(g)$ and $V(g)$ are two representations of the group element g in a group G, then the complement channel is covariant in the following form:

$$\Phi^c[U(g)\rho U^\dagger(g)] = \Omega^\dagger(g)\Phi^c(\rho)\Omega(g) \quad \forall\, g \in G, \tag{26}$$

where $\Omega(g)$ is the representation defined in the following form:

$$V^\dagger(g)K_i U(g) = \sum_j \Omega_{i,j}(g)K_j. \tag{27}$$

2. Complementary channel of Λ_x

The formula (24) gives a very simple recipe for writing the Kraus operators of the complementary channel easily. Put the first rows of all the Kraus operators in consecutive rows of a matrix and call it R_1, put the second rows of all the Kraus operators in consecutive rows of a matrix and call it R_2, and so on and so forth. Since the Kraus operators of the channel Λ_x are given by

$$K_0 = \sqrt{1-x}\begin{bmatrix} 1 & 0 & 0 \\ 0 & 1 & 0 \\ 0 & 0 & 1 \end{bmatrix} \tag{28}$$

and

$$K_1 = -i\sqrt{\frac{x}{2}}\begin{bmatrix} 0 & 0 & 0 \\ 0 & 0 & 1 \\ 0 & -1 & 0 \end{bmatrix}, \quad K_2 = -i\sqrt{\frac{x}{2}}\begin{bmatrix} 0 & 0 & -1 \\ 0 & 0 & 0 \\ 1 & 0 & 0 \end{bmatrix}, \quad K_3 = -i\sqrt{\frac{x}{2}}\begin{bmatrix} 0 & 1 & 0 \\ -1 & 0 & 0 \\ 0 & 0 & 0 \end{bmatrix}, \tag{29}$$

it is readily found that the Kraus operators of Λ_x^c are given by

$$R_1 = \begin{bmatrix} \sqrt{1-x} & 0 & 0 \\ 0 & 0 & 0 \\ 0 & 0 & i\sqrt{x/2} \\ 0 & -i\sqrt{x/2} & 0 \end{bmatrix}, \quad R_2 = \begin{bmatrix} 0 & \sqrt{1-x} & 0 \\ 0 & 0 & -i\sqrt{x/2} \\ 0 & 0 & 0 \\ i\sqrt{x/2} & 0 & 0 \end{bmatrix}, \quad R_3 = \begin{bmatrix} 0 & 0 & \sqrt{1-x} \\ 0 & i\sqrt{x/2} & 0 \\ -i\sqrt{x/2} & 0 & 0 \\ 0 & 0 & 0 \end{bmatrix}. \tag{30}$$

In passing and for future use, it is instructive to note the effect of the complementary channel on a general matrix

$$X = \begin{pmatrix} a & b & c \\ d & e & f \\ g & h & k \end{pmatrix}, \tag{31}$$

which is readily found from (30) to be

$$\Lambda_x^c(X) = \frac{1}{2}\begin{pmatrix} 2(1-x)[(a+e+k)] & i\sqrt{2x(1-x)}(f-h) & -i\sqrt{2x(1-x)}(c-g) & i\sqrt{2x(1-x)}(b-d) \\ i\sqrt{2x(1-x)}(f-h) & x(e+k) & -dx & -gx \\ -i\sqrt{2x(1-x)}(c-g) & -bx & x(a+k) & -hx \\ i\sqrt{2x(1-x)}(b-d) & -cx & -fx & x(a+e) \end{pmatrix}. \tag{32}$$

In the case of channel Λ_x, we have

$$U^\dagger K_0 U = K_0, \quad U^\dagger K_i U = \sum_j U_{ij} K_j, \quad U \in \mathrm{SO}(3), \tag{33}$$

where $U = e^{i\theta \mathbf{n}\cdot\mathbf{J}}$ is the spin-1 representation of a rotation. Hence,

$$\Omega = \begin{pmatrix} 1 & \mathbf{0}^T \\ \mathbf{0} & U \end{pmatrix}. \tag{34}$$

Therefore, the channel Λ_x^c is also covariant under SU(3) when $x = 0$ and is covariant under SO(3) for arbitrary x.

IV. DEGRADABILITY AND ANTIDEGRADABILITY

Degradable and antidegradable channels belong to a noteworthy class of completely positive trace-preserving maps. These channels possess advantageous properties that we use in this paper to analyze various capacities.

Definition 1. [43,52] Let $\mathcal{E} : A \longrightarrow B$ and $\mathcal{E}^c : A \longrightarrow E$ be a quantum channel and its complement, respectively. Then, $\mathcal{E}$ is degradable if there exists a quantum channel $\mathcal{N} : B \longrightarrow E$, such that $\mathcal{N} \circ \mathcal{E}(\rho) = \mathcal{E}^c(\rho)$. It is antidegradable if there exists a quantum channel $\mathcal{M} : E \longrightarrow B$ such that $\mathcal{M} \circ \mathcal{E}^c(\rho) = \mathcal{E}(\rho)$, Fig. 1.

We first note that in the specific point $x = 1$, where we have the pure Landau-Streater channel and $K_0 = 0$, $K_{1,2,3} = J_{x,y,z}$, it is readily seen that the Kraus operators R_i will be 3×3 matrices and

$$R_1 = -K_1, \quad R_2 = -K_2, \quad R_3 = -K_3. \tag{35}$$

That is, the Landau-Streater channel and its complement are the same,

$$\Lambda_1(\rho) = \Lambda_1^c(\rho). \tag{36}$$

This implies that the Landau-Streater channel is both degradable and antidegradable simultaneously and has important implications for the quantum capacity of the channel, as we will later explain. In the other extreme, when $x = 0$ and we have the identity channel, $\Lambda_0(\rho) = \rho$, we find

$$\begin{aligned} R_1 &= (1, 0, 0) = |0\rangle\langle 1|, \\ R_2 &= (0, 1, 0) = |0\rangle\langle 2|, \\ R_3 &= (0, 0, 1) = |0\rangle\langle 3|, \end{aligned} \tag{37}$$

which leads to

$$\Lambda_0^c(\rho) = \mathrm{tr}(\rho)|0\rangle\langle 0|. \tag{38}$$

It is then obvious that the channel is degradable with $\mathcal{N}(\rho) = \mathrm{tr}(\rho)|0\rangle\langle 0|$, since $\Lambda_0^c(\rho) = (\mathcal{N} \circ \Lambda)(\rho)$, and since no channel can retrieve a state from its trace, the channel Λ_x is not antidegradable at point $x = 0$.

V. CAPACITIES OF THE NOISY LANDAU-STREATER CHANNEL

We have now concluded our partial investigation of the properties of channel Λ_x. In this section, our focus shifts to the examination of its various capacities. Calculating different capacities analytically is not always feasible, except in some special cases [53–63]. We leverage the symmetry properties of this channel to derive analytical expressions for its Holevo quantity and entanglement-assisted capacity. We then numerically find upper and lower bounds for the quantum capacity and determine the region of nonzero quantum capacity. This is shown in Fig. 4. Let us start with the classical capacity.

A. Classical capacity

The classical capacity represents the ultimate rate at which classical messages can be faithfully transmitted through a channel upon being encoded into quantum states. This concept is formulated as [64,65]

$$C_{cl}(\Phi) = \lim_{n\longrightarrow\infty} \frac{1}{n} \chi^*(\Phi^{\otimes n}), \tag{39}$$

where $\chi^*(\Phi)$ is defined as

$$\chi^*(\Phi) = \max_{p_i, \rho_i} S\left(\sum_i p_i \Phi(\rho_i)\right) - \sum_i p_i S[\Phi(\rho_i)].$$

In this context, the von Neumann entropy is represented as $S(\rho) = -\mathrm{Tr}(\rho \log \rho)$ [66]. It is crucial to note that χ^* exhibits superadditivity, meaning that $n\chi^*(\Phi) \leqslant \chi^*(\Phi^{\otimes n})$. This necessitates the regularization step in Eq. (39) for calculation of the classical capacity [67].

1. The Holevo quantity

This regularization being extremely difficult, we, as many others [46,68,69], try to calculate the Holevo quantity, which is a lower bound on the regularized classical capacity, that is,

$$\chi^*(\Phi) \leqslant C_{cl}(\Phi). \tag{40}$$

Since channel Λ_x is irreducibly covariant, we can use a result of Holevo [70], according to which $\chi^*(\Lambda_x)$ is given by

$$\chi^*(\Lambda_x) = \log_2 d - \min_\rho S[\Lambda_x(\rho)]. \tag{41}$$

Thus, our task reduces to finding the minimum output entropy state of channel Λ_x. As entropy is a concave function, we know that this minimum output state can be taken to be a pure state [35]. To find this minimum output entropy state, we use the covariance properties of the channel. First, consider the two endpoints of the parameter space $\{0, 1\}$, namely, $x = 0$ and $x = 1$. In these two points, the channel has SU(3) covariance, which means that if a given state $|\psi_0\rangle$ is a minimum output entropy state, so is the state $U|\psi_0\rangle$, where U is an arbitrary $U \in \mathrm{SU}(3)$. This is due to the fact that

$$S[\Lambda_i(U\rho U^\dagger)] = S[U\Lambda_i(\rho)U^\dagger] = S[\Lambda_i(\rho)], \quad i = 0, 1. \tag{42}$$

We can now use this full SU(3) covariance to choose the minimum output entropy state as

$$\rho_{\min} = |1\rangle\langle 1|, \quad \text{where} \quad |1\rangle = \begin{pmatrix} 1 \\ 0 \\ 0 \end{pmatrix}. \tag{43}$$

This immediately leads to

$$\Lambda_0(|1\rangle\langle 1|) = \begin{pmatrix} 1 & 0 & 0 \\ 0 & 0 & 0 \\ 0 & 0 & 0 \end{pmatrix}, \quad \Lambda_1(|1\rangle\langle 1|) = \begin{pmatrix} 0 & 0 & 0 \\ 0 & 1 & 0 \\ 0 & 0 & 1 \end{pmatrix}, \tag{44}$$

from which we obtain

$$\chi^*(\Lambda_0) = \log_2 3, \quad \chi^*(\Lambda_1) = \log_2 3 - 1. \tag{45}$$

However, when x is not an endpoint, the channel's full SU(3) covariance is broken down to its SO(3) subgroup. It is no longer possible to transform any arbitrary state in the complex Hilbert space H_3 to a fixed state like $|1\rangle$ by SO(3) rotations. To use this limited covariance, suppose that the minimum output entropy state is given by

$$|\Psi\rangle = \begin{pmatrix} \psi_1 \\ \psi_2 \\ \psi_3 \end{pmatrix}, \tag{46}$$

where ψ_1, ψ_2, and ψ_3 are complex numbers, modulo the normalization condition and a global phase. We now use a group element $O_1 \in \mathrm{SO}(3)$ with a suitable rotation parameter α,

$$O_1 = \begin{pmatrix} \cos\alpha & \sin\alpha & 0 \\ -\sin\alpha & \cos\alpha & 0 \\ 0 & 0 & 1 \end{pmatrix}, \tag{47}$$

to make ψ_2 real [i.e., we can always choose α so that $\mathrm{Im}(-\psi_1 \sin\alpha + \psi_2 \cos\alpha) = 0$] and turn $|\Psi\rangle$ to

$$|\Psi\rangle = \begin{pmatrix} \psi_1 \\ r_2 \\ \psi_3 \end{pmatrix}, \quad r_2 \in R. \tag{48}$$

With another rotation of the form

$$O_2 = \begin{pmatrix} \cos\beta & 0 & \sin\beta \\ 0 & 1 & 0 \\ -\sin\beta & 0 & \cos\beta \end{pmatrix}, \tag{49}$$

with a suitable parameter β, we can make ψ_3 also real,

$$|\Psi\rangle = \begin{pmatrix} \psi_1 \\ r_2 \\ r_3 \end{pmatrix}, \quad r_2,\ r_3 \in R. \tag{50}$$

Finally, we use the rotation matrix $O_3 \in \mathrm{SO}(3)$

$$O_3 = \begin{pmatrix} 1 & 0 & 0 \\ 0 & \cos\gamma & \sin\gamma \\ 0 & -\sin\gamma & \cos\gamma \end{pmatrix} \tag{51}$$

to eliminate the third component $(-r_2 \sin\gamma + r_3 \cos\gamma = 0)$ and set the form of $|\Psi\rangle$ into

$$|\Psi\rangle = \begin{pmatrix} \cos\theta e^{i\phi} \\ \sin\theta \\ 0 \end{pmatrix}, \tag{52}$$

where normalization has also been used. The output of the channel Λ_x is now given by

$$\Lambda_x(|\Psi\rangle\langle\Psi|) = \begin{pmatrix} (1-x)\cos^2\theta + \frac{x}{2}\sin^2\theta & \cos\theta\sin\theta\big[(1-x)e^{i\phi} - \frac{x}{2}e^{-i\phi}\big] \\ \cos\theta\sin\theta\big[(1-x)e^{i\phi} - \frac{x}{2}e^{-i\phi}\big] & (1-x)\sin^2\theta + \frac{x}{2}\cos^2\theta \end{pmatrix} \oplus \frac{x}{2} I_1. \tag{53}$$

Let us abbreviate the above matrix to $\Lambda_x(|\Psi\rangle\langle\Psi|) = M \oplus \frac{x}{2} I_1$. Then, the eigenvalues of this matrix are $\frac{x}{2}$ plus the two eigenvalues of the matrix M. Instead of explicit calculation of the eigenvalues of M, which we denote as λ_1 and λ_2, we note that

$$\mathrm{tr}(M) \equiv \lambda_1 + \lambda_2 = 1 - \frac{x}{2}, \quad \mathrm{Det}(M) \equiv \lambda_1\lambda_2 = \frac{1}{2}x(1-x)(1 - \sin^2 2\theta \sin^2\phi). \tag{54}$$

The sum of eigenvalues is fixed and independent of the input state $|\Psi\rangle$. The minimum output entropy is obtained when the two eigenvalues are as far apart as possible, i.e., when $\mathrm{Det}(M)$ is a minimum that is realized for

$$\theta = \frac{\pi}{4}, \quad \phi = \frac{\pi}{2}. \tag{55}$$

This leads to $\mathrm{Det}(M) = 0$. Thus, the minimum output entropy state is

$$|\Psi\rangle = \frac{1}{\sqrt{2}} \begin{pmatrix} i \\ 1 \\ 0 \end{pmatrix}, \tag{56}$$

and the eigenvalues of M are $\{\lambda_1 = 0,\ \lambda_2 = 1 - \frac{x}{2}\}$. Taking into account the third eigenvalue $\lambda_3 = \frac{x}{2}$, the minimum output entropy will be

$$S = -\frac{x}{2}\log_2\frac{x}{2} - \left(1 - \frac{x}{2}\right)\log_2\left(1 - \frac{x}{2}\right), \tag{57}$$

which leads to

$$\chi^*(\Lambda_x) = \log_2 3 + \frac{x}{2}\log_2\frac{x}{2} + \left(1 - \frac{x}{2}\right)\log_2\left(1 - \frac{x}{2}\right), \tag{58}$$

which, in view of (58), shows that the classical capacity is a continuous function of the parameter x. Figure 3 shows the Holevo quantity as a function of x.

2. Upper bound for classical capacity

We employ an upper bound using semidefinite programming, as introduced in Ref. [71] and denoted as C_β. Consider a quantum channel $\Phi : A \to B$, where $J(\Phi) = \sum_{ij}(|i\rangle\langle j|) \otimes (\Phi(|i\rangle\langle j|))$ to represent its Choi matrix [72]. Take S_B and R as Hermitian matrices in B and $A \otimes B$, respectively. Then, it is shown that [71]

$$C_{cl}(\Phi) \leqslant C_\beta(\Phi) := \log_2[\min_{\Delta} \mathrm{Tr}(S_B)],$$

where the subscript Δ is meant to denote the constraints on S_B in this optimization, which is to be performed over all feasible Hermitian matrices S_B and R, subject to

$$-R \leqslant J(\Phi)^{T_B} \leqslant R$$
$$-I_A \otimes S_B \leqslant R^{T_B} \leqslant I_A \otimes S_B.$$

Here, T_B signifies the partial transpose operation with respect to subspace B, defined as $(|ij\rangle\langle kl|)^{T_B} = |il\rangle\langle kj|$. We utilize

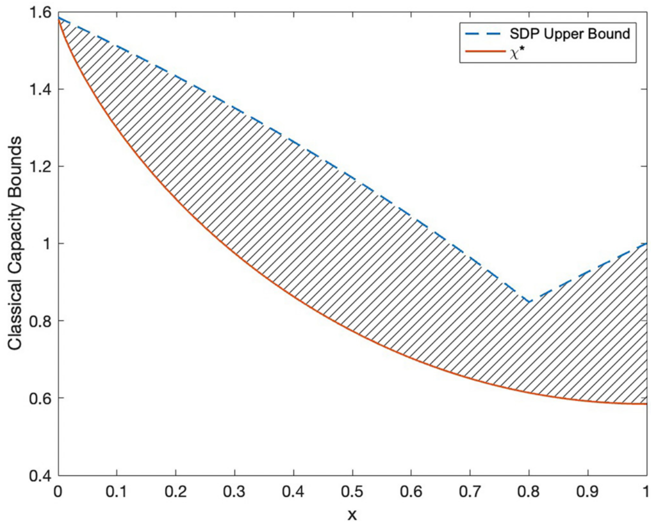

FIG. 2. The Holevo quantity χ^* and classical capacities' semidefinite programming (SDP) upper bound of channel Λ_x as a function of x. The shaded region shows the allowable region for the classical capacity of the channel. When $x = 0$, i.e., the identity channel, the upper and lower bounds are equal to $\log_2(3)$. The parameter x and the quantity χ^* are dimensionless. The parameter x and the capacities are dimensionless.

this method to establish an upper bound for the classical capacity of the channel (5), as visually represented in Fig. 2.

B. Entanglement-assisted capacity

Entanglement-assisted capacity is a measure of the maximum rate at which quantum information can be transmitted through a noisy quantum channel when the sender and receiver are allowed to share an entangled quantum state [73]. The entanglement-assisted classical capacity of a channel Φ is determined by [74]

$$C_{ea}(\Phi) = \max_{\rho} I(\rho, \Phi), \tag{59}$$

where

$$I(\rho, \Phi) := S(\rho) + S[\Phi(\rho)] - S(\rho, \Phi). \tag{60}$$

Here, $S(\rho, \Phi)$ is the output entropy of the environment, referred to as the entropy exchange [75], and is represented by the expression $S(\rho, \Phi) = S[\Phi_x^c(\rho)]$, where Φ_x^c is the complementary channel [see Sec. (III B)]. According to Proposition 9.3 in Ref. [76], the maximum entanglement-assisted capacity of a covariant channel Φ is attained for an invariant state ρ. In the special case where Φ is irreducibly covariant, the maximum is attained on the maximally mixed state. Hence, for the channel (5),

$$C_{ea}(\Lambda_x) = S\left(\frac{I}{3}\right) + S\left[\Lambda_x\left(\frac{I}{3}\right)\right] - S\left[\Lambda_x^c\left(\frac{I}{3}\right)\right], \tag{61}$$

which, given the unitarity of the channel, leads to

$$\begin{aligned} C_{ea}(\Lambda_x) &= 2S\left(\frac{I}{3}\right) - S\left[\Lambda_x^c\left(\frac{I}{3}\right)\right] \\ &= 2\log_2 3 - S\left[\Lambda_x^c\left(\frac{I}{3}\right)\right]. \end{aligned} \tag{62}$$

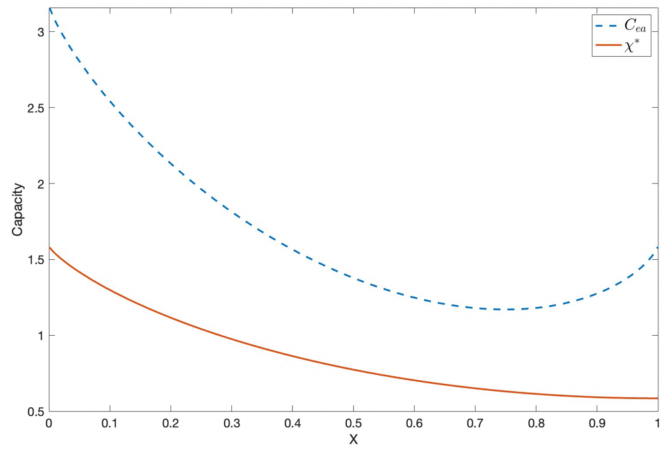

FIG. 3. The Holevo quantity χ^* and entanglement assisted (C_{ea}) capacities of channel Λ_x as a function of x. All quantities and parameters are dimensionless.

From (32), one finds

$$\Lambda_x^c\left(\frac{I}{3}\right) = \begin{pmatrix} 1-x & 0 & 0 & 0 \\ 0 & \frac{x}{3} & 0 & 0 \\ 0 & 0 & \frac{x}{3} & 0 \\ 0 & 0 & 0 & \frac{x}{3} \end{pmatrix},$$

which gives the final expression for the entanglement-assisted classical capacity,

$$C_{ea}(\Lambda_x) = 2\log_2 3 + x\log_2\frac{x}{3} + (1-x)\log_2(1-x). \tag{63}$$

The specific limiting points of the graph (3) can be understood on physical grounds as follows. First, consider the point $x = 0$, where the channel is identity. In this case, without using entanglement, we can communicate the classical bits 0, 1, and 2, by encoding them into the qutrit states $|0\rangle$, $|1\rangle$, and $|-1\rangle$, which after passing through the channel can be retrieved in a safe form. This will give mutual information of

$$\begin{aligned} I_{cl,x=0}(X;Y) &\equiv H(X) - H(X|Y) \\ &= \log_2 3 - 0 = \log_2 3 \approx 1.58. \end{aligned} \tag{64}$$

When $x = 0$, we can run the usual dense-coding protocol and communicate two classical traits by sending each single qutrit through the channel. This gives the mutual information $I_{ea,x=0} = H(X) - H(X|Y) = \log_2 9 = 2\log_2 3 \approx 3.17$, as shown in Fig. 3. At the other endpoint, when $x = 1$, we calculate the mutual information as follows. Let us use the same encoding $(0,\ 1,\ 2) \longrightarrow |0\rangle,\ |1\rangle,\ |-1\rangle)$. Call an arbitrary qutrit state $|m\rangle$ and send it through the channel. This turns into the mixed state

$$\Lambda_1(|m\rangle\langle m|) = \tfrac{1}{2}(I - |m\rangle\langle m|),$$

and is received by the receiver. A projective measurement by the receiver leads to the following pattern of conditional probabilities: $P(y = m|x = m) = 0$ and $P(y \neq m|x = m) = \frac{1}{2}$. This gives the following mutual information:

$$I_{cl,x=1}(X:Y) = H(X) - H(X|Y) = \log_2 3 - 1 \approx 0.58. \tag{65}$$

It remains to make a concrete calculation of C_{ea} at $x = 1$. This is the most nontrivial, and we have only found examples that are compatible with the results in Fig. 3. In Appendix A, we explain two different protocols that yield different mutual information, both compatible with the result (63). Figure 3 shows both classical and entanglement-assisted capacity as a function of x.

C. Quantum capacity

The largest rate at which quantum information can be sent reliably through a quantum channel Φ is represented by its quantum capacity $Q(\Phi)$. The coherent information $I_c(\Phi, \rho) = S[\Phi(\rho)] - S[\Phi^c(\rho)]$ is an entropic quantity that can be used to express the quantum capacity. The maximum value of I_c over all input states ρ is denoted by $Q_1(\Phi)$, i.e.,

$$Q_1(\Phi) = \max_{\rho} I_c(\Phi, \rho) = \max_{\rho} S[\Phi(\rho)] - S[\Phi^c(\rho)]. \quad (66)$$

To define the quantum capacity of a channel, $Q(\Phi)$, we use the single-letter quantum capacity and take the limit as n approaches infinity [75,77,78]:

$$\lim_{n\to\infty} \frac{1}{n} Q_1(\Phi^{\otimes n}). \quad (67)$$

When the channel Φ is degradable, this regularization is not necessary, and we have

$$Q(\Phi) = Q_1(\Phi), \quad (68)$$

and calculation of $Q_1(\Phi)$ is then a convex optimization problem. In general, however, performing the regularization in (67) is extremely difficult, if not impossible [79]; even for very simple qubit channels like the depolarizing or the Pauli channel, determining the quantum capacity remains elusive [80]. This is because of the superadditivity of coherent information, i.e., for two quantum channels, denoted as Φ_1 and Φ_2, the coherent information of the joint channel $\Phi_1 \otimes \Phi_2$ satisfies a specific inequality [81–83],

$$Q_1(\Phi_1 \otimes \Phi_2) \geqslant Q_1(\Phi_1) + Q_1(\Phi_2), \quad (69)$$

and this inequality can be strict [61,67,83–87]. Consequently, bounding techniques are commonly used to obtain upper and lower bounds on the quantum capacity [44,45,51,84]. In this paper, we review some bounding techniques that are efficiently computable and then apply them to our channel (5). These bounds are not monotone as a function of the parameter x. Consequently, we invoke two different bounds from the combination of which we will find a rather narrow region for the quantum capacity of this channel.

1. Semidefinite programming upper bound of quantum capacity

A general upper bound for quantum capacity using semidefinite programming is introduced in Ref. [80] and is denoted by Q_Γ. Let $\Phi : A \to B$, be a quantum channel and let $J(\Phi) = \sum_{ij} (|i\rangle\langle j|) \otimes [\Phi(|i\rangle\langle j|)]$ be its Choi matrix [72]. Let ρ_A be an arbitrary density matrix in A and R be an arbitrary positive semidefinite linear operator in $L^+(A \otimes B)$. Then, it is shown that [80]

$$Q(\Phi) \leqslant Q_\Gamma(\Phi) := \log_2 \{\max\ \mathrm{Tr}[J(\Phi)R]\}, \quad (70)$$

where maximization is done on the set of all density matrices ρ_A and all positive semidefinite matrices R subject to the condition

$$-\rho_A \otimes I_B \leqslant R^{T_B} \leqslant \rho_A \otimes I_B,$$

where T_B represents the partial transpose operation with respect to space B, defined as $(|ij\rangle\langle kl|)^{T_B} = |il\rangle\langle kj|$. In this paper, we will use this method to upper bound the quantum capacity of the channel (5).

2. Flagged extension upper bound

Flagged extension is a technique that has proven to be effective for finding upper bounds on the quantum capacity of various quantum channels. It involves constructing a new channel with a higher-dimensional output Hilbert space for any channel that can be expressed as a convex combination of other channels. While this technique does not provide a general upper bound and requires specific settings to be tight and computable, it has been successful in investigating the quantum capacities of several channels [44,45,57,87]. In this section, we use two different flagged extensions and obtain two different upper bounds for the quantum channel which complement each other.

a. Flagged extension with orthogonal flags. An upper bound for the quantum capacity of a quantum channel can be found using the following theorem, which is the result of a flagged extension of degradable channels with orthogonal flags. The theorem was first proved in Ref. [87].

Theorem 1. [87] Suppose we have

$$\Phi = \sum_i p_i \Phi_i,$$

where Φ_i is degradable for all i. The following inequality holds:

$$Q(\Phi) \leqslant \sum_i p_i Q(\Phi_i) = \sum_i p_i Q_1(\Phi_i), \quad (71)$$

where the last equality is due to the degradability assumption of all Φ_is.

Channel Λ_x is already in a convex form $\Lambda_x = (1 - x)\Lambda_0(\rho) + x\Lambda_1(\rho)$, where Λ_0 and Λ_1 are both degradable (see Sec. IV). This allows a simple upper bound to be found by using the above theorem. Since the Λ_1 channel is known to be antidegradable [see the discussion after Eq. (36)], its quantum capacity is zero. We simply obtain

$$Q(\Lambda_x) \leqslant (1 - x)Q_1(\Lambda_0) + xQ_1(\Lambda_1), \quad (72)$$

since Λ_1 is antidegradable $Q_1(\Lambda_1) = 0$, and $Q_1(\Lambda_0) = 0$ being the quantum capacity of the identity channel, is simply found from

$$\begin{aligned} Q_1(\Lambda_0) &= \max_{\rho} \left\{S[\Lambda_0(\rho)] - S\left[\Lambda_0^c(\rho)\right]\right\} \\ &= \max_{\rho} \{S(\rho) - S[\mathrm{tr}(\rho)]\} = \max_{\rho} S(\rho) = \log_2 3, \end{aligned} \quad (73)$$

which leads to

$$Q(\Lambda_x) \leqslant (1 - x)Q_1(\Lambda_0) = (1 - x)\log_2 3. \quad (74)$$

In Fig. 4, we denote this upper bound as Q_{f1}.

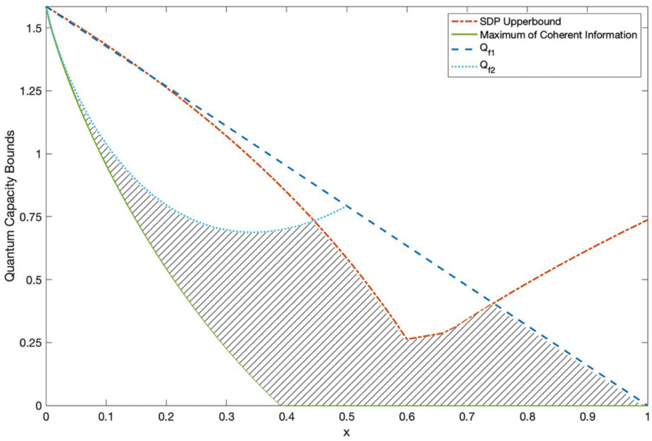

FIG. 4. Various bounds for the generalized Landau-Streater channel are presented. The figure illustrates that the flagged extension upper bound Q_{f2} performs optimally in the region $0 \leqslant x \leqslant 0.4435$, while the SDP upper bound excels in the region $0.4435 \leqslant x \leqslant 0.75$. In the remaining regions, the flagged extension upper bound Q_{f1} outperforms other bounds. The hatched area in the figure signifies the potential quantum capacity values. The lower bound for the quantum capacity, the green solid line, is obtained both by a numerical search as in (77) and by taking an ansatz for this optimum state as in (78). The results agree. Moreover the lower bound is zero for $x = 1$, which conforms with the antidegradability of the channel Λ_1. The parameter x and the quantum capacity are dimensionless.

b. Flagged extension with nonorthogonal flags. An alternative degradable flagged extension of the channel (5) for $0 \leqslant x \leqslant \frac{1}{2}$, can be achieved through [57]

$$\mathbb{\Lambda}_x(\rho) = (1-x)\rho \otimes |\phi_0\rangle\langle\phi_0| + x\Lambda_1(\rho) \otimes |\phi_1\rangle\langle\phi_1|, \tag{75}$$

where

$$|\phi_0\rangle = \sqrt{\frac{1-2x}{1-x}}|0\rangle + \sqrt{\frac{x}{1-x}}|1\rangle, \quad |\phi_1\rangle = |0\rangle.$$

This results in

$$Q(\Lambda_x) \leqslant Q(\mathbb{\Lambda}_x) = Q_1(\mathbb{\Lambda}_x),$$

with the last equality arising from the degradability of the flagged extension channel. Notably, the covariance of this channel remains SO(3). Let us denote the covariance group of this channel as G, and assume that U_g for $g \in G$ is an irreducible representation of this group. By exploiting the irreducible covariance of the channel (75), we have

$$\frac{1}{|G|}\sum_{g\in G} U_g \rho U_g^{\dagger} = \frac{I}{d}, \tag{76}$$

where d is the dimension of the input space of the channel (in this case, $d = 3$). Moreover, due to the degradability of the flagged extension channel, the coherent information is concave. By leveraging the invariance of the coherent information under the covariance of the channel, we obtain

$$I_c\left(\mathbb{\Lambda}_x, \frac{I}{3}\right) = I_c\Big(\mathbb{\Lambda}_x, \frac{1}{|G|}\sum_{g\in G} U_g\rho U_g^{\dagger}\Big) \geqslant \frac{1}{|G|}\sum_{g\in G} I_c(\mathbb{\Lambda}_x, U_g\rho U_g^{\dagger})$$
$$= I_c(\mathbb{\Lambda}_x, \rho),$$

where $|G|$ is the cardinality of the group G. The inequality comes from the concavity of the coherent information, and the equality is due to Eq. (76). Hence,

$$Q_1(\mathbb{\Lambda}_x) = \max_{\rho} I_c(\mathbb{\Lambda}_x, \rho) = I_c\left(\mathbb{\Lambda}_x, \frac{I}{3}\right).$$

Therefore, it is sufficient to evaluate $I_c(\mathbb{\Lambda}_x, \frac{I}{3}) = S[\mathbb{\Lambda}_x(\frac{I}{3})] - S(\mathbb{\Lambda}_x \otimes I\,|\phi^+\rangle\langle\phi^+|)$, where $|\phi^+\rangle = \frac{1}{3}\sum_{i=0}^{3}|ii\rangle$. In this regard, first, we calculate $S[\mathbb{\Lambda}_x(\frac{I}{3})]$:

$$S\left[\mathbb{\Lambda}_x\left(\frac{I}{3}\right)\right] = S\left(\frac{I}{3} \otimes [(1-x)|\phi_0\rangle\langle\phi_0| + x|\phi_1\rangle\langle\phi_1|]\right)$$
$$= \log(3) + S[(1-x)|\phi_0\rangle\langle\phi_0| + x|\phi_1\rangle\langle\phi_1|].$$

Now, we should calculate $S(\mathbb{\Lambda}_x \otimes I\,|\phi^+\rangle\langle\phi^+|)$. The nonzero eigenvalues of $J(\mathbb{\Lambda}_x)$ are $(1-x, \frac{x}{3}, \frac{x}{3}\frac{x}{3})$ (see Appendix B), hence,

$$S[J(\mathbb{\Lambda}_x)] = -(1-x)\log_2(1-x) - x\log_2\left(\frac{x}{3}\right).$$

We have visualized and labeled this upper bound as Q_{f2} in Fig. 4. We have found (not reported here for simplicity) that for our channel and all values of the parameter x, the bounds introduced here are lower than the other upper bounds introduced in the literature, like the partial transposition bound [88], which is efficiently computable by SDP [89,90]. Therefore, to obtain a reasonable upper bound for all values of the parameter x, we only need to compare the flag-extension upper bounds and the SDP bound.

D. Lower bound for the quantum capacity

In order to restrict the allowable values of the quantum capacity, we also need a lower bound. Due to the superadditivity of the channel [i.e., $Q_1(\Phi) \leqslant \frac{1}{n}Q_1(\Phi^{\otimes n})$], a natural lower bound for $Q(\Lambda_x)$ is given by $Q_1(\Lambda_x)$. This is given by

$$Q_1(\Lambda_x) = \max_{\rho} I_c(\Lambda_x, \rho). \tag{77}$$

The optimization problem in inequality (77) can be evaluated using various numerical methods. Here, we adopt a hybrid strategy that combines the capabilities of the "fmincon" local optimization algorithm and the GlobalSearch global optimization algorithm, both accessible through MATLAB's Optimization Toolbox and Global Optimization Toolbox. This approach is tailored to effectively address the challenges posed by our nonconvex optimization problem. It is worth noting that our problem is mathematically equivalent to minimizing the negative of the coherent information, expressed as $-\min_{\rho} -I_c(\Lambda_x, \rho)$. Therefore, we address this optimization problem, which necessitates finding minima. GlobalSearch expands the search scope by initially sampling points within the solution space. It then uses "fmincon" to fine-tune and identify local minima in these initial points.

We can also follow a semianalytical method which confirms this numerical result. Let us take an ansatz for ρ of the form $\rho_0 = \mathrm{diag}(s, 1-2s, s)$, where s is a real parameter. In view of (77), it is true that

$$\max_{s} I_c(\Lambda_x, \rho_0) \leqslant Q_1(\Lambda_x) \leqslant Q(\Lambda_x). \tag{78}$$

The optimization over this single parameter can then be performed numerically, the result of which coincides with the one performed by the previously mentioned toolbox. We obtain that for x less than 0.38, $s = \frac{1}{3}$, which means that $\rho_0 = \frac{I}{3}$, and for x greater than 0.38, $I_c(\Lambda, \frac{I}{3})$ becomes negative and hence will not be a meaningful lower bound. For this region, we find the lower bound is actually equal to zero, which is achieved by any of the following pure states: $|1\rangle := (1, 0, 0)^T$, $|0\rangle := (0, 1, 0)^T$, and $|-1\rangle := (0, 0, 1)^T$. In fact, one sees from (5) and (32) that

$$\Lambda_x(|1\rangle\langle 1|) = \begin{pmatrix} 1-x & & \\ & \frac{x}{2} & \\ & & \frac{x}{2} \end{pmatrix}, \quad (79)$$

and

$$\Lambda_x^c(|1\rangle\langle 1|) = \begin{pmatrix} 1-x & & & \\ & 0 & & \\ & & \frac{x}{2} & \\ & & & \frac{x}{2} \end{pmatrix}, \quad (80)$$

both of which have the same entropy, thus leading to $I_c(\Lambda_x, |1\rangle\langle 1|) = 0$. The same thing happens for the other two pure states. This lower bound precisely coincides with the result obtained through numerical search.

Combining the two upper bounds, namely, the SDP upper bound and the flag-extension upper bound and the lower bound $Q_1(\Lambda_x)$, we find the hashed area in Fig. 4 for the allowable values of the quantum capacity of the channel Λ_x.

VI. ANTIDEGRADABILITY OF CHANNEL Λ_x FOR $\frac{4}{7} \leqslant x \leqslant 1$

It is clear that the Holevo-Werner or the Landau-Streater channel Λ_1 is both degradable and antidegradable and hence its quantum capacity is zero. The question arises whether these two properties still hold for a certain period near $x = 1$. In this section we show that channel Λ_x is antidegradable in the interval $\frac{4}{7} \leqslant x \leqslant 1$. Hence, in this interval, channel Λ_x has zero quantum capacity. In view of the superadditivity of the quantum channel and the extreme difficulty of its calculation, this is a significant result. To prove this statement, we find a channel $\mathcal{N}$ such that

$$\Lambda_x(\rho) = \mathcal{N}\big[\Lambda_x^c(\rho)\big].$$

First, let us remind the reader about the fundamental representation of SO(3) generators that we used and the Kraus operators of the complementary channel Λ_c. With k, l, and $m \in \{1, 2, 3\}$ in cyclic order, we have from (29) and (30) that

$$\begin{aligned} J_m &= -i(|k\rangle\langle l| - |l\rangle\langle k) \\ R_k &= \sqrt{1-x}|0\rangle\langle k| - \sqrt{\frac{x}{2}}J_k, \\ k &= 1, 2, 3. \end{aligned} \quad (81)$$

Note that the Kraus operators R_k are 4×3 dimensional matrices with rows indexed by 0,1,2, and 3 and columns indexed by 1,2, and 3. We now define the channel $\mathcal{N}$ by the following 3×4 dimensional Kraus operators:

$$N_0 = t\sum_{i=1}^{3}|i\rangle\langle i| = tI_3, \quad N_k = \frac{1}{\sqrt{3}}|k\rangle\langle 0| - rJ_k, \quad k = 1, 2, 3, \quad (82)$$

where I_3 and J_k are the embedding of the three-dimensional matrices in the corresponding blocks of the matrices, i.e.,

$$N_0 = (0 \quad tI_3) \quad N_k = \left(\frac{1}{\sqrt{3}}|k\rangle \quad -rJ_k\right).$$

The parameter r is chosen to satisfy

$$r\sqrt{\frac{x}{2}} = \sqrt{\frac{1-x}{3}}, \quad (83)$$

and t is a real parameter to be determined (note that the phase of a complex t can always be removed to make it real, without affecting the definition of the channel). A simple calculation shows that

$$N_0^\dagger N_0 + \sum_{k=0}^{3} N_k^\dagger N_k = |0\rangle\langle 0| + (t^2 + 2r^2)I_3, \quad (84)$$

where the requirement of trace preserving demands that

$$t^2 + 2r^2 = 1. \quad (85)$$

We also need the following simply proved identity:

$$J_k J_l = \delta_{kl} I_3 - |l\rangle\langle k|. \quad (86)$$

It is then a simple matter to use (83) and show that

$$\begin{aligned} N_0 R_k &= -t\sqrt{\frac{x}{2}}J_k, \\ N_k R_k &= \sqrt{\frac{1-x}{3}}|k\rangle\langle k| + r\sqrt{\frac{x}{2}}J_k^2 \\ &= \sqrt{\frac{1-x}{3}}|k\rangle\langle k| + r\sqrt{\frac{x}{2}}(I_3 - |k\rangle\langle k|) = \sqrt{\frac{1-x}{3}}I_3 \\ N_k R_l &= \sqrt{\frac{1-x}{3}}|k\rangle\langle l| + r\sqrt{\frac{x}{2}}J_k J_l \\ &= \sqrt{\frac{1-x}{3}}|k\rangle\langle l| - r\sqrt{\frac{x}{2}}|l\rangle\langle k| = i\sqrt{\frac{1-x}{3}}J_m, \end{aligned} \quad (87)$$

where we have noted the cyclic order of the indices $(k, \ l, \ m)$. We can now evaluate $\mathcal{N}[\Lambda_x^c(\rho)]$:

$$\begin{aligned} \mathcal{N}\big[\Lambda_x^c(\rho)\big] &= \sum_{k=0,l=1}^{3} N_k R_l(\rho)(N_k R_l)^\dagger \\ &= \sum_k (N_0 R_k)(\rho)(N_0 R_k)^\dagger + \sum_k (N_k R_k)(\rho)(N_k R_k)^\dagger \\ &\quad + \sum_{k\neq l}(N_k R_l)(\rho)(N_k R_l)^\dagger \\ &= \frac{x}{2}t^2\sum_k J_k\rho J_k^\dagger + (1-x)\rho \\ &\quad + \frac{2}{3}(1-x)\sum_m J_m\rho J_m^\dagger \\ &= (1-x)\rho + \left[\frac{x}{2}t^2 + \frac{2}{3}(1-x)\right]\sum_k J_k\rho J_k^\dagger. \end{aligned} \quad (88)$$

The right-hand side will be the same as $\Lambda_x(\rho)$, if t satisfies

$$\frac{x}{2}t^2 + \frac{2}{3}(1-x) = \frac{x}{2}, \tag{89}$$

which in view of (83) is the same as the trace-preserving condition. This requires that the parameter t satisfies

$$t^2 = \frac{7x-4}{3x}, \tag{90}$$

which means that in the region $\frac{4}{7} \leqslant x \leqslant 1$, the channel is antidegradable and hence its quantum capacity is zero.

VII. CONCLUSION AND OUTLOOK

Until now, the Werner-Holevo or Landau-Streater channel, being an extreme point in the space of qutrit channels, has been of interest only due to its structural properties. We have shown that when suitably modified, this channel can in fact be looked at as a familiar noise model on three-level states. The noise consists of random rotations in different directions by arbitrary angles. In view of the wider interest [7,12–24,26–34] in qutrits as a potential candidate for quantum information processing, our result may find applications in modeling realistic noise on qutrits. The interesting point is that the action of these continuous random rotations can be represented by three simple Kraus operators. This puts our channel on the same footing for qutrits as the depolarizing channel for qubits.

The difference with the familiar depolarizing channel is that the latter does not have a simple Kraus representation in terms of physicality. We have then proceeded to determine many of the physical properties of this channel, including its various capacities, where we have found exact expressions for the Holevo quantity, the entanglement-assisted capacity, and upper and lower bounds for its quantum capacity.

Our work can be extended in a number of ways. The first one reveals itself when we look at Eqs. (14). It is readily seen that the coefficient a cannot be zero, and in fact, the smallest value of this coefficient is $\frac{1}{15}$, which is achieved when all the rotations are equal to $\pm\frac{\pi}{2}$. This is the closest distance that we can come to the Werner-Holevo channel by random unitary rotations. The question of how close we can come to an extreme point by random unitary operations is an open question, not only for the Werner-Holevo channel but for any extreme point of CPT maps in general. This problem can be pursued further if we study the higher-spin representations of the Landau-Streater channel, or even by generalizing the Landau-Streater channel so that we replace the generators of SO(3) with those of the SO(d) group. This channel is completely different from the Landau-Streater channel, i.e., it has $d(d-1)/2$ Kraus operators in d dimensions but is still equivalent to the Werner-Holevo channel, and consequently it is SU(d) covariant. These are open problems that remain for future publications.

ACKNOWLEDGMENT

This research was supported in part by Iran National Science Foundation, under Grant No. 4022322. The authors wish to thank V. Jannessary, M. Nobakht, A. Farmanian, A. Najafzadeh, A. Tangestani, L. Memarzadeh, A. Rezakhani, S. Oskuie, and M. Mirkamali for their valuable comments and suggestions.

APPENDIX A: PROTOCOLS FOR ENTANGLEMENT-ASSISTED CLASSICAL COMMUNICATION

In this Appendix, we propose two different protocols for dense coding via the Werner-Holevo channel (3) and calculate the corresponding mutual information. In the first protocol, we let the entangled state $|\Phi\rangle_{AB} = \frac{1}{\sqrt{3}}(|00\rangle + |11\rangle + |22\rangle)$ be shared between the two players, whom we call Alice (A) and Bob (B). Alice encodes her trit $n = 0,\ 1,\ 2$ into the entangled state by acting on her share of the state by Z^n, where $Z = \begin{pmatrix} 1 & & \\ & \omega & \\ & & \omega^2 \end{pmatrix}$, where $\omega^3 = 1$, and in this way encodes her trit m into

$$|\Phi_n\rangle_{AB} = \frac{1}{\sqrt{3}}(|00\rangle + \omega^n|11\rangle + \omega^{2n}|22\rangle.$$

When her share passes through the channel, Bob will find the complete state to be

$$\begin{aligned}\rho_n &= (\Lambda_1 \otimes I)|\Phi_n\rangle\langle\Phi_n| \\ &= \frac{1}{3}(\Lambda_1 \otimes I)\sum_{j,k}\omega^{(j-k)n}|j,j\rangle\langle k,k| \\ &= \frac{1}{3}\sum_{j,k}\omega^{(j-k)n}\Lambda_1(|j\rangle\langle k|)\otimes|j\rangle\langle k| \\ &= \frac{1}{6}\sum_{j,k}\omega^{(j-k)n}(\delta_{j,k}I - |k\rangle\langle j|)\otimes|j\rangle\langle k| \\ &= \frac{1}{6}\left(I\otimes I - \sum_{j,k}\omega^{(j-k)n}|k,j\rangle\langle j,k|\right).\end{aligned} \tag{A1}$$

Now that Bob has the full state ρ_n, he has the task of determining the index n by an optimum measurement. It is not so easy to find this optimal measurement, or maybe there are better protocols for encoding classical trites into entangled states and sending it to Bob. In the present protocol, one possible measurement is the following positive operator valued measure (POVM):

$$E_p = \sum_{l=0}^{2}|l,l+p\rangle\langle l,l+p| \quad p = 0,\ 1,\ 2. \tag{A2}$$

A straightforward calculation then shows that

$$P(y=p|x=n) \equiv \mathrm{tr}(E_p\rho_n) = \tfrac{1}{2}(1-\delta_{p,n}). \tag{A3}$$

This leads to mutual information

$$\begin{aligned}I(X:Y) &= H(X) + H(Y) - H(X,Y) \\ &= \log_2 3 + \log_2 3 - \log_2 6 \\ &= \log_2 3 - 1,\end{aligned} \tag{A4}$$

which is below the analytical value $C_{ea,x=1}(\Lambda_x) = \log_2 3$. Another dense coding protocol is that Alice performs a unitary operator Z^nX^m on the entangled state $|\Phi\rangle_{AB}$ and turns it into one of the nine maximally entangled Bell states, hence encoding two classical trits (m,n) into this state and sending her own qutrit to Bob (through the channel Λ_{LS}), who will make a Bell measurement and determine the classical pair of trits (m, n). However, detailed calculation shows that the mutual information in this scenario is again equal to $\log_2 3 - 1$. Therefore, it is an interesting problem to see what kind of protocol saturates the value $C_{ea} = \log_2 3$.

APPENDIX B: EIGENVALUES OF $(\mathbb{A}_x \otimes I\,|\phi^+\rangle\langle\phi^+|)$

In this Appendix, we evaluate the eigenvalues of the Choi matrix of the flagged extension channel with nonorthogonal flags. To achieve this we expand $(\mathbb{A}_x \otimes I)\,|\phi^+\rangle\langle\phi^+|$ as follows:

$$(\mathbb{A}_x \otimes I)\,|\phi^+\rangle\langle\phi^+| = \frac{1}{3}\sum_{i,j=1}^{3}\left[(1-x)|i\rangle\langle j| \otimes |\phi_0\rangle\langle\phi_0| \otimes |i\rangle\langle j| + \frac{x}{2}\sum_{\alpha=1}^{3} J_\alpha|i\rangle\langle j|J_\alpha \otimes |\phi_1\rangle\langle\phi_1| \otimes |i\rangle\langle j|\right].$$

Since $|i\rangle\langle j|$, $|\phi_0\rangle\langle\phi_0| \otimes |i\rangle\langle j|$, $J_\alpha|i\rangle\langle j|J_\alpha$, and $|\phi_1\rangle\langle\phi_1| \otimes |i\rangle\langle j|$ are all square matrices, there exists a permutation matrix Q such that

$$(\mathbb{A}_x \otimes I)\,|\phi^+\rangle\langle\phi^+| = \frac{1}{3}\sum_{i,j=1}^{3} Q\left[(1-x)|\phi_0\rangle\langle\phi_0| \otimes |i\rangle\langle j| \otimes |i\rangle\langle j| + \frac{x}{2}\sum_{\alpha=1}^{3} |\phi_1\rangle\langle\phi_1| \otimes |i\rangle\langle j| \otimes J_\alpha|i\rangle\langle j|J_\alpha\right]Q^T.$$

Now we define $|J_\alpha\rangle = \frac{1}{2}\sum_i |i\rangle \otimes J_\alpha|i\rangle$; with this definition we can write the above equation in a simpler form:

$$(\mathbb{A}_x \otimes I)\,|\phi^+\rangle\langle\phi^+| = Q\left[(1-x)|\phi_0\rangle\langle\phi_0| \otimes |\phi^+\rangle\langle\phi^+| + \frac{x}{3}\sum_{\alpha=1}^{3} |\phi_1\rangle\langle\phi_1| \otimes |J_\alpha\rangle\langle J_\alpha|\right]Q^T.$$

Now observe that $\langle J_\alpha|J_\beta\rangle = \mathrm{Tr}(J_\alpha^\dagger J_\beta) = \delta_{\alpha\beta}$ and $\langle J_\alpha|\phi^+\rangle = \mathrm{Tr}(J_\alpha^\dagger) = 0$, which indicates that the eigenvalues of $(\mathbb{A}_x \otimes I)\,|\phi^+\rangle\langle\phi^+|$ are $(1-x, \frac{x}{3}, \frac{x}{3}, \frac{x}{3})$.

[1] R. F. Werner and A. S. Holevo, Counterexample to an additivity conjecture for output purity of quantum channels, J. Math. Phys. **43**, 4353 (2002).

[2] A. I. Pakhomchik, I. Feshchenko, A. Glatz, V. M. Vinokur, A. V. Lebedev, S. N. Filippov, and G. B. Lesovik, Realization of the Werner–Holevo and Landau–Streater quantum channels for qutrits on quantum computers, J. Russ. Laser Res. **41**, 40 (2020).

[3] L. J. Landau and R. F. Streater, On Birkhoff's theorem for doubly stochastic completely positive maps of matrix algebras, Linear Algebra Appl. **193**, 107 (1993).

[4] K. M. R. Audenaert and S. Scheel, On random unitary channels, New J. Phys. **10**, 023011 (2008).

[5] C. M. Caves and G. J. Milburn, Qutrit entanglement, Opt. Commun. **179**, 439 (2000).

[6] D. Bruß and C. Macchiavello, Optimal eavesdropping in cryptography with three-dimensional quantum states, Phys. Rev. Lett. **88**, 127901 (2002).

[7] G. Molina-Terriza, A. Vaziri, R. Ursin, and A. Zeilinger, Experimental quantum coin tossing, Phys. Rev. Lett. **94**, 040501 (2005).

[8] V. M. Kendon, K. Życzkowski, and W. J. Munro, Bounds on entanglement in qudit subsystems, Phys. Rev. A **66**, 062310 (2002).

[9] N. J. Cerf, S. Massar, and S. Pironio, Greenberger-Horne-Zeilinger paradoxes for many qudits, Phys. Rev. Lett. **89**, 080402 (2002).

[10] S. D. Bartlett, H. de Guise, and B. C. Sanders, Quantum encodings in spin systems and harmonic oscillators, Phys. Rev. A **65**, 052316 (2002).

[11] J. Bouda and V. Buzek, Entanglement swapping between multi-qudit systems, J. Phys. A: Math. Gen. **34**, 4301 (2001).

[12] E. Karimi, S. A. Schulz, I. D. Leon, H. Qassim, J. Upham, and R. W. Boyd, Generating optical orbital angular momentum at visible wavelengths using a plasmonic metasurface, Light Sci. Appl. **3**, e167 (2014).

[13] L. Marrucci, E. Karimi, S. Slussarenko, B. Piccirillo, E. Santamato, E. Nagali, and F. Sciarrino, Spin-to-orbital conversion of the angular momentum of light and its classical and quantum applications, J. Opt. **13**, 064001 (2011).

[14] A. Sit *et al.*, High-dimensional intracity quantum cryptography with structured photons, Optica **4**, 1006 (2017).

[15] E. Nagali, F. Sciarrino, F. De Martini, L. Marrucci, B. Piccirillo, E. Karimi, and E. Santamato, Quantum information transfer from spin to orbital angular momentum of photons, Phys. Rev. Lett. **103**, 013601 (2009).

[16] Y. Wang, Z. Hu, B. C. Sanders, and S. Kais, Qudits and high-dimensional quantum computing, Front. Phys. **8**, 589504 (2020).

[17] D. M. Hugh and J. Twamley, Trapped-ion qutrit spin molecule quantum computer, New J. Phys. **7**, 174 (2005).

[18] A. B. Klimov, R. Guzmán, J. C. Retamal, and C. Saavedra, Qutrit quantum computer with trapped ions, Phys. Rev. A **67**, 062313 (2003).

[19] Y. I. Bogdanov, M. V. Chekhova, S. P. Kulik, G. A. Maslennikov, A. A. Zhukov, C. H. Oh, and M. K. Tey, Qutrit state engineering with biphotons, Phys. Rev. Lett. **93**, 230503 (2004).

[20] S. Gröblacher, T. Jennewein, A. Vaziri, G. Weihs, and A. Zeilinger, Experimental quantum cryptography with qutrits, New J. Phys. **8**, 75 (2006).

[21] B. P. Lanyon, T. J. Weinhold, N. K. Langford, J. L. O'Brien, K. J. Resch, A. Gilchrist, and A. G. White, Manipulating biphotonic qutrits, Phys. Rev. Lett. **100**, 060504 (2008).

[22] C. Schaeff, R. Polster, M. Huber, S. Ramelow, and A. Zeilinger, Experimental access to higher-dimensional entangled quantum systems using integrated optics, Optica **2**, 523 (2015).

[23] A. Babazadeh, M. Erhard, F. Wang, M. Malik, R. Nouroozi, M. Krenn, and A. Zeilinger, High-dimensional single-photon quantum gates: Concepts and experiments, Phys. Rev. Lett. **119**, 180510 (2017).

[24] H.-H. Lu, Z. Hu, M. S. Alshaykh, A. J. Moore, Y. Wang, P. Imany, A. M. Weiner, and S. Kais, Quantum phase estimation with time–frequency qudits in a single photon, Adv. Quantum Technol. **3**, 1900074 (2020).

[25] S. Dogra, Arvind, and K. Dorai, Determining the parity of a permutation using an experimental NMR qutrit, Phys. Lett. A **378**, 3452 (2014).

[26] T. Bækkegaard, L. B. Kristensen, N. J. S. Loft, C. K. Andersen, D. Petrosyan, and N. T. Zinner, Realization of efficient quantum gates with a superconducting qubit-qutrit circuit, Sci. Rep. **9**, 13389 (2019).

[27] R. Bianchetti, S. Filipp, M. Baur, J. M. Fink, C. Lang, L. Steffen, M. Boissonneault, A. Blais, and A. Wallraff, Control and tomography of a three-level superconducting artificial atom, Phys. Rev. Lett. **105**, 223601 (2010).

[28] S. Danilin, A. Vepsäläinen, and G. S. Paraoanu, Experimental state control by fast non-Abelian holonomic gates with a superconducting qutrit, Phys. Scr. **93**, 055101 (2018).

[29] M. A. Yurtalan, J. Shi, M. Kononenko, A. Lupascu, and S. Ashhab, Implementation of a Walsh-Hadamard gate in a superconducting qutrit, Phys. Rev. Lett. **125**, 180504 (2020).

[30] M. Kononenko, M. A. Yurtalan, S. Ren, J. Shi, S. Ashhab, and A. Lupascu, Characterization of control in a superconducting qutrit using randomized benchmarking, Phys. Rev. Res. **3**, L042007 (2021).

[31] J. Randall, S. Weidt, E. D. Standing, K. Lake, S. C. Webster, D. F. Murgia, T. Navickas, K. Roth, and W. K. Hensinger, Efficient preparation and detection of microwave dressed-state qubits and qutrits with trapped ions, Phys. Rev. A **91**, 012322 (2015).

[32] J. Lindon, A. Taschilina, L. W. Cooke, and L. J. LeBlanc, Complete unitary qutrit control in ultracold atoms, Phys. Rev. Appl. **19**, 034089 (2023).

[33] P. J. Low, B. M. White, A. A. Cox, M. L. Day, and C. Senko, Practical trapped-ion protocols for universal qudit-based quantum computing, Phys. Rev. Res. **2**, 033128 (2020).

[34] M. Ringbauer, M. Meth, L. Postler, R. Stricker, R. Blatt, P. Schindler, and T. Monz, A universal qudit quantum processor with trapped ions, Nat. Phys. **18**, 1053 (2022).

[35] M. M. Wilde, *Quantum Information Theory* (Cambridge University Press, Cambridge, 2017).

[36] B. Misra and E. C. G. Sudarshan, The Zeno's paradox in quantum theory, J. Math. Phys. **18**, 756 (1977).

[37] J. M. Raimond, P. Facchi, B. Peaudecerf, S. Pascazio, C. Sayrin, I. Dotsenko, S. Gleyzes, M. Brune, and S. Haroche, Quantum Zeno dynamics of a field in a cavity, Phys. Rev. A **86**, 032120 (2012).

[38] J. M. Raimond, C. Sayrin, S. Gleyzes, I. Dotsenko, M. Brune, S. Haroche, P. Facchi, and S. Pascazio, Phase space tweezers for tailoring cavity fields by quantum Zeno dynamics, Phys. Rev. Lett. **105**, 213601 (2010).

[39] C. Bayındır and F. Ozaydin, Freezing optical rogue waves by Zeno dynamics, Opt. Commun. **413**, 141 (2018).

[40] C. Bayındır, Zeno dynamics of quantum chirps, Phys. Lett. A **389**, 127096 (2021).

[41] P. Horodecki, M. Horodecki, and R. Horodecki, Bound entanglement can be activated, Phys. Rev. Lett. **82**, 1056 (1999).

[42] F. Ozaydin, C. Bayindir, A. A. Altintas, and C. Yesilyurt, Nonlocal activation of bound entanglement via local quantum Zeno dynamics, Phys. Rev. A **105**, 022439 (2022).

[43] I. Devetak and P. W. Shor, The capacity of a quantum channel for simultaneous transmission of classical and quantum information, Commun. Math. Phys. **256**, 287 (2005).

[44] M. Fanizza, F. Kianvash, and V. Giovannetti, Quantum flags and new bounds on the quantum capacity of the depolarizing channel, Phys. Rev. Lett. **125**, 020503 (2020).

[45] M. Fanizza, F. Kianvash, and V. Giovannetti, Estimating quantum and private capacities of Gaussian channels via degradable extensions, Phys. Rev. Lett. **127**, 210501 (2021).

[46] S. N. Filippov and K. V. Kuzhamuratova, Quantum informational properties of the Landau–Streater channel, J. Math. Phys. **60**, 042202 (2019).

[47] M. M. Wolf and J. I. Cirac, Dividing quantum channels, Commun. Math. Phys. **279**, 147 (2008).

[48] W. F. Stinespring, Positive functions on C^*-algebras, Proc. Am. Math. Soc. **6**, 211 (1955).

[49] N. Datta, M. Fukuda, and A. S. Holevo, Complementarity and additivity for covariant channels, Quantum Info. Proc. **5**, 179 (2006).

[50] M. Smaczyński, W. Roga, and K. Życzkowski, Self-complementary quantum channels, Open Syst. Inf. Dyn. **23**, 1650014 (2016).

[51] A. Poshtvan and V. Karimipour, Capacities of the covariant Pauli channel, Phys. Rev. A **106**, 062408 (2022).

[52] T. S. Cubitt, M. B. Ruskai, and G. Smith, The structure of degradable quantum channels, J. Math. Phys. **49**, 102104 (2008).

[53] C. King, The capacity of the quantum depolarizing channel, IEEE Trans. Inf. Theory **49**, 221 (2003).

[54] C. H. Bennett, D. P. DiVincenzo, and J. A. Smolin, Capacities of quantum erasure channels, Phys. Rev. Lett. **78**, 3217 (1997).

[55] G. Smith, J. A. Smolin, and A. Winter, The quantum capacity with symmetric side channels, IEEE Trans. Inf. Theory **54**, 4208 (2008).

[56] Y. Ouyang, Channel covariance, twirling, contraction and some upper bounds on the quantum capacity, Quantum Inf. Comput. **14**, 917 (2014).

[57] F. Kianvash, M. Fanizza, and V. Giovannetti, Bounding the quantum capacity with flagged extensions, Quantum **6**, 647 (2022).

[58] S. Chessa and V. Giovannetti, Quantum capacity analysis of multi-level amplitude damping channels, Commun. Phys. **4**, 22 (2021).

[59] A. Arqand, L. Memarzadeh, and S. Mancini, Quantum capacity of a bosonic dephasing channel, Phys. Rev. A **102**, 042413 (2020).

[60] S. K. Oskouei, S. Mancini, and A. Winter, Capacities of Gaussian quantum channels with passive environment assistance, IEEE Trans. Inf. Theory **68**, 339 (2022).

[61] F. Leditzky, D. Leung, and G. Smith, Quantum and private capacities of low-noise channels, Phys. Rev. Lett. **120**, 160503 (2018).
[62] S. Chessa and V. Giovannetti, Resonant multilevel amplitude damping channels, Quantum **7**, 902 (2023).
[63] S. Chessa and V. Giovannetti, Partially coherent direct sum channels, Quantum **5**, 504 (2021).
[64] B. Schumacher and M. D. Westmoreland, Sending classical information via noisy quantum channels, Phys. Rev. A **56**, 131 (1997).
[65] A. S. Holevo, The capacity of the quantum channel with general signal states, IEEE Trans. Inf. Theory **44**, 269 (1998).
[66] M. A. Nielsen and I. L. Chuang, *Quantum Computation and Quantum Information* (Cambridge University Press, Cambridge, 2010).
[67] M. B. Hastings, Superadditivity of communication capacity using entangled inputs, Nat. Phys. **5**, 255 (2009).
[68] A. D'Arrigo, G. Benenti, G. Falci, and C. Macchiavello, Classical and quantum capacities of a fully correlated amplitude damping channel, Phys. Rev. A **88**, 042337 (2013).
[69] V. Giovannetti and R. Fazio, Information-capacity description of spin-chain correlations, Phys. Rev. A **71**, 032314 (2005).
[70] A. S. Holevo, Remarks on the classical capacity of quantum channel, arXiv:quant-ph/0212025.
[71] X. Wang, W. Xie, and R. Duan, Semidefinite programming strong converse bounds for classical capacity, IEEE Trans. Inf. Theory **64**, 640 (2018).
[72] M.-D. Choi, Completely positive linear maps on complex matrices, Linear Algebra Appl. **10**, 285 (1975).
[73] C. H. Bennett, P. W. Shor, J. A. Smolin, and A. V. Thapliyal, Entanglement-assisted classical capacity of noisy quantum channels, Phys. Rev. Lett. **83**, 3081 (1999).
[74] C. H. Bennett, P. W. Shor, J. A. Smolin, and A. V. Thapliyal, Entanglement-assisted capacity of a quantum channel and the reverse Shannon theorem, IEEE Trans. Inf. Theory **48**, 2637 (2002).
[75] H. Barnum, M. A. Nielsen, and B. Schumacher, Information transmission through a noisy quantum channel, Phys. Rev. A **57**, 4153 (1998).
[76] A. S. Holevo, *Quantum Systems, Channels, Information: A Mathematical Introduction*, Number 16 in De Gruyter studies in mathematical physics (De Gruyter, Berlin, 2012).
[77] S. Lloyd, Capacity of the noisy quantum channel, Phys. Rev. A **55**, 1613 (1997).
[78] I. Devetak, The private classical capacity and quantum capacity of a quantum channel, IEEE Trans. Inf. Theory **51**, 44 (2005).
[79] T. Cubitt, D. Elkouss, W. Matthews, M. Ozols, D. Pérez-García, and S. Strelchuk, Unbounded number of channel uses may be required to detect quantum capacity, Nat. Commun. **6**, 6739 (2015).
[80] X. Wang and R. Duan, A semidefinite programming upper bound of quantum capacity, in *Proceedings of the 2016 IEEE International Symposium on Information Theory (ISIT)* (Barcelona, Spain, 2016), pp. 1690–1694.
[81] P. W. Shor and J. A. Smolin, Quantum error-correcting codes need not completely reveal the error syndrome, arXiv:quant-ph/9604006.
[82] F. Leditzky, D. Leung, V. Siddhu, G. Smith, and J. A. Smolin, The platypus of the quantum channel zoo, in *2022 IEEE International Symposium on Information Theory (ISIT)* (Barcelona, Spain, 2016), pp. 1690–1694.
[83] D. P. DiVincenzo, P. W. Shor, and J. A. Smolin, Quantum-channel capacity of very noisy channels, Phys. Rev. A **57**, 830 (1998).
[84] J. Fern and K. B. Whaley, Lower bounds on the nonzero capacity of Pauli channels, Phys. Rev. A **78**, 062335 (2008).
[85] J. Bausch and F. Leditzky, Error thresholds for arbitrary Pauli noise, SIAM J. Comput. **50**, 1410 (2021).
[86] V. Siddhu and R. B. Griffiths, Positivity and nonadditivity of quantum capacities using generalized erasure channels, IEEE Trans. Inf. Theory **67**, 4533 (2021).
[87] G. Smith and J. A. Smolin, Additive extensions of a quantum channel, *2008 IEEE Information Theory Workshop* (IEEE, Piscataway, NJ, 2008).
[88] A. Holevo and R. Werner, Evaluating capacities of bosonic Gaussian channels, Phys. Rev. A **63**, 032312 (2001).
[89] J. Watrous, Semidefinite programs for completely bounded norms, arXiv:0901.4709 [quant-ph].
[90] J. Watrous, Simpler semidefinite programs for completely bounded norms, arXiv:1207.5726 [quant-ph].